

---

# GAN2GAN: Generative Noise Learning for Blind Image Denoising with Single Noisy Images

---

Sungmin Cha, Taeon Park and Taesup Moon  
Department of Electrical and Computer Engineering  
Sungkyunkwan University  
Suwon, Korea 16419  
{csm9493, pte1236, tsmoon}@skku.edu

## Abstract

We tackle a challenging blind image denoising problem, in which only single noisy images are available for training a denoiser and no information about noise is known, except for it being zero-mean, additive, and independent of the clean image. In such a setting, which often occurs in practice, it is not possible to train a denoiser with the standard discriminative training or with the recently developed Noise2Noise (N2N) training; the former requires the underlying clean image for the given noisy image, and the latter requires two independently realized noisy image pair for a clean image. To that end, we propose GAN2GAN (Generated-Artificial-Noise to Generated-Artificial-Noise) method that can first learn to generate synthetic noisy image pairs that simulate independent realizations of the noise in the given images, then carry out the N2N training of a denoiser with those synthetically generated noisy image pairs. Our method consists of three parts: extracting smooth noisy patches to learn the noise distribution in the given images, training a generative model to synthesize the noisy image pairs, and devising an iterative N2N training of a denoiser. In results, we show the denoiser trained with our GAN2GAN, solely based on single noisy images, achieves an impressive denoising performance, almost approaching the performance of the standard discriminatively-trained or N2N-trained models that have more information than ours, and significantly outperforming the recent baselines for the same setting.

## 1 Introduction

Image denoising is one of the oldest problems in image processing and low-level computer vision, yet it still attracts lots of attention due to the fundamental nature of the problem. Vast number of algorithms have been proposed over the past several decades, and recently, the CNN-based methods [4] [23] [20] [15] became the throne-holders in terms of the PSNR performance.

The main approach of the most CNN-based denoisers is to apply the discriminative learning framework with the *known* noise distribution assumption. Namely, it assumes to first have the *clean* images and generates the (clean, noisy) image pairs by corrupting the clean images with the known noise, *e.g.*, additive Gaussian noise with zero-mean and known  $\sigma$ . Then, the CNN is used to learn the denoising mapping from the obtained supervised training set.

While being effective, above approach also possesses a couple of limitations that become critical in practice. Firstly, the known noise assumption may not always hold. For example, it is likely that the standard deviation,  $\sigma$ , of the Gaussian noise is not known *a priori*, or the noise may not always follow the Gaussian distribution. In such cases, the mismatch between the trained CNN denoiser and the given noisy data would occur, which can significantly deteriorate the denoising performance. Secondly, obtaining the noise-free clean images, necessary for building the supervised training set, is

not always possible or very expensive depending on the applications, *e.g.*, medical imaging (CT or MRI) or astrophotographs.

Several attempts have been made to resolve above issues. For the noise uncertainty, the so-called *blind training* have been proposed. Namely, thanks to the robustness of neural networks, a denoiser can be trained with a composite training set that contains images corrupted with multiple, predefined noise levels or distributions. The blindly trained denoisers were shown to alleviate the mismatch scenarios mentioned above to some extent, but the second limitation, *i.e.*, the requirement of noise-free clean images for building the training set, still remains. As an attempt to address this second limitation, the Noise2Noise (N2N) [13] method has been recently proposed. Namely, it has been shown that the denoisers can be trained without the clean target images, as long as two independent noisy image realizations for the same underlying clean image are available. Their results were impressive that the denoising performance of the N2N trained model showed almost negligible difference compared to the ordinary supervised trained model with the clean target images. However, the requirement of the *two* independently realized noisy image pair for a single clean image, which may hardly be available in practice, is a limiting factor for the N2N framework.

In this paper, we tackle the two limitations at the same time, *i.e.*, we consider the complete unsupervised blind denoising setting where only *single* noisy images are available. Namely, in our setting, nothing is known about the noise other than it being zero-mean, additive, and independent of the clean image, and neither the clean target images nor the noisy image pairs are available. The crux of our method is to learn Wasserstein GAN [1]-based generative models that can learn and simulate the noise distribution of the observed noisy images, then can generate synthetic noisy image pairs for each of the given underlying (unobserved) clean image. The generated noisy image pairs are then used for training a CNN denoiser as in N2N. Our resulting method is dubbed as GAN2GAN (Generated-Artificial-Noise to Generated-Artificial-Noise), and we show that the denoising performance of GAN2GAN trained model almost approaches those of the standard discriminatively-trained or N2N-trained models on a widely used benchmark dataset, BSD68 with Gaussian noise. Moreover, our scheme is shown to significantly outperform a recent work that considered the same setting, Noise2Void [12], on various different kinds of noise, *e.g.*, mixture or correlated noise.

## 2 Related Work

**Deep learning-based denoisers** Following the pioneering work [11], the deep learning-based, particularly, the CNN-based denoisers [4, 23, 20, 15] achieved the state-of-the-art PSNR performance by employing the discriminative training framework. Again, we stress that most of those models typically require to know the noisy variance and the clean target images for training. The blindly-trained denoiser was first proposed in [23] as well to alleviate the known noise assumption, and their DnCNN-B model was shown to almost achieve the noise-matched model as long as the noise variance in the given noisy image falls in the range of variances in the composite training set. Several other work on blind denoising beyond building a composite dataset have been also proposed. For example, [24] incorporated an end-point control framework for finding the right level of noise in the image. Moreover, [5] devised a scheme to learn and generate noise in the given noisy images using Generative Adversarial Networks (GAN) and utilized the unpaired clean images to build a supervised training set. Our work is closely related to [5], but we improve their noise learning process and do not use the clean data at all.

**Denoising only with the noisy images** As mentioned in the Introduction, [13] recently proposed Noise2Noise (N2N) that pioneered the idea of training a denoiser solely with noisy images. The limitation of their work is the requirement of the noisy image pair for a single image. More recently, [2][12] extended N2N and proposed methods that can train a denoiser only with single noisy images, namely, Noise2Self and Noise2Void, respectively. Their settings exactly coincide with ours, but we show our method significantly outperforms their methods. More classical denoising methods typically are capable of denoising solely based on the single noisy images applying various different principles, such as filtering-based [3, 6], optimization-based [8, 17, 10], Wavelet transform-based [7], and effective prior-based methods [27]. More recently, several work proposed to implement deep learning-based priors or regularizers, such as [21, 22, 16], but their PSNR still could not compete with the supervised trained CNN-based denoisers.

**Generative Adversarial Nets (GAN)** GAN [9] have made tremendous impacts in generative learning, and we only list the two most relevant work here. Wasserstein GAN [1] (W-GAN) replaced

the binary-classification based discriminator of the original GAN with a “critic” that measures the distributional similarity between the true and generated data using the Wasserstein distance. CycleGAN [26] devised a notion of cycle consistency to transform a source image to a one with only the intended feature changed, while maintaining other structures of the image intact. We combine these two recently developed ideas for our blind image denoising problem.

### 3 GAN2GAN: Generative Noise Learning from Single Noisy Images

#### 3.1 Notations and problem setting

We assume the noisy image  $\mathbf{Z}$  is generated by  $\mathbf{Z} = \mathbf{x} + \mathbf{N}$ , in which  $\mathbf{x}$  denotes the underlying clean image and  $\mathbf{N}$  denotes the zero-mean, additive noise that is independent of  $\mathbf{x}$ . For training the denoiser, we do not assume that neither the distribution nor the covariance of  $\mathbf{N}$  is known. Moreover, we assume only  $n$  noisy images for *distinct* clean images,  $\mathcal{D} = \{\mathbf{Z}^{(i)}\}_{i=1}^n$ , are available for learning the denoiser, hence, a straightforward N2N training is not possible. The CNN-based denoiser is denoted as  $\hat{\mathbf{X}}_{\theta}(\mathbf{Z})$ , in which  $\theta$  is the model parameters, and we use the standard quality metrics, PSNR and SSIM, to evaluate the goodness of denoising. Furthermore, following the convention, we normalize the pixels of the images to have values in  $[0, 1]$ .

#### 3.2 Description of GAN2GAN

The primary motivation of GAN2GAN is simple; given a single noisy image  $\mathbf{Z}^{(i)}$ , we want to generate two image pairs  $(\hat{\mathbf{Z}}_1^{(i)}, \hat{\mathbf{Z}}_2^{(i)})$  that correspond to the noisy images for the same underlying clean image of  $\mathbf{Z}^{(i)}$ , but each with independent realization of the noise that is present in  $\mathbf{Z}^{(i)}$ . Such generation is challenging, since we have to blindly separate the noise and the clean image solely from  $\mathbf{Z}^{(i)}$ , learn the distribution of the noise, and switch only the noise part of  $\mathbf{Z}^{(i)}$  with the independent realizations of the noise. Despite the challenge, once successful, we can then use those pairs to carry out the N2N training to train a denoiser. To achieve this goal, we propose the following 3 steps of our GAN2GAN.

##### 3.2.1 Smooth noisy patch extraction

The first step is to extract the noisy image patches from  $\mathcal{D}$  that correspond to smooth, homogeneous areas. Then, by exploiting the fact that the noise is zero-mean and additive, we can subtract the mean of each patch to obtain the patches of pure “noise”. Such noise patches are then used to train a W-GAN that can simulate the noise, as described in the next subsection.

Our extraction method is based on the GCBD method proposed in [5], but we make an important improvement. The GCBD determines a patch  $\mathbf{p}$  is smooth if it satisfies the following rules for all of its smaller sub-patches,  $\mathbf{q}_j$ :

$$|\mathbb{E}(\mathbf{q}_j) - \mathbb{E}(\mathbf{p})| \leq \mu \mathbb{E}(\mathbf{p}) \text{ and } |\mathbf{Var}(\mathbf{q}_j) - \mathbf{Var}(\mathbf{p})| \leq \gamma \mathbf{Var}(\mathbf{p}), \quad (1)$$

in which  $\mathbb{E}(\cdot)$  and  $\mathbf{Var}(\cdot)$  stand for the empirical mean and variance of the pixel values in a patch, and  $\mu, \gamma \in (0, 1)$  are the hyperparameters for the rule.

While the rule (1) works for extracting smooth patches to some extent, we show in our experiments that it also ends up choosing patches with high-frequency repeating patterns, which are far from true noise. Thus, we instead utilize 2D discrete Wavelet transform (DWT) for a new extraction rule. Namely, we determine a patch  $\mathbf{p}$  is smooth if its four sub-band decompositions obtained by DWT,  $\{W_1(\mathbf{p}), W_2(\mathbf{p}), W_3(\mathbf{p}), W_4(\mathbf{p})\}$ , satisfy the following condition:

$$\frac{1}{4} \sum_{k=1}^4 \left| \mathbf{Var}(W_k(\mathbf{p})) - \mathbb{E}[\mathbf{Var}_W(\mathbf{p})] \right| \leq \lambda \mathbb{E}[\mathbf{Var}_W(\mathbf{p})], \quad (2)$$

in which  $\mathbb{E}[\mathbf{Var}_W(\mathbf{p})] \triangleq \frac{1}{4} \sum_{k=1}^4 \mathbf{Var}(W_k(\mathbf{p}))$  and  $\lambda \in (0, 1)$ . Thus, in words, if the empirical variance of the coefficients of each of the four sub-bands is not far from the average of them, we determine  $\mathbf{p}$  is a smooth patch. This single rule is much simpler than (1), which has to be evaluated for all the sub-patches. In the experimental results, we show this modification of the extraction rule plays a critical role in our GAN training and the final denoising performance. Once  $N$  smooth noisy patches are extracted from  $\mathcal{D}$  using (2), we subtract each patch with its mean pixel value, and obtain

a set of “noise” patches,  $\mathcal{N} = \{\mathbf{n}^{(j)}\}_{j=1}^N$ . Such subtraction is valid since in smooth patches, all the pixel values should be close to their mean.

### 3.2.2 Training W-GANs to simulate noisy images

Equipped with the noisy images  $\mathcal{D} = \{\mathbf{Z}^{(i)}\}_{i=1}^n$  and the extracted noise patches  $\mathcal{N} = \{\mathbf{n}^{(j)}\}_{j=1}^N$ , we train a W-GAN based generative model as shown in Figure 1. The model has three generators,  $\{g_{\theta_1}, g_{\theta_2}, g_{\theta_3}\}$ , and two critics,  $\{f_{w_1}, f_{w_2}\}$ , and the subscripts stand for the model parameters.

The loss functions associated with the components of our model are following

$$\mathcal{L}_n(\theta_1, w_1) \triangleq \mathbb{E}_n[f_{w_1}(\mathbf{n})] - \mathbb{E}_r[f_{w_1}(g_{\theta_1}(\mathbf{r}))] \quad (3)$$

$$\mathcal{L}_Z(\theta_1, \theta_2, w_2) \triangleq \mathbb{E}_Z[f_{w_2}(\mathbf{Z})] - \mathbb{E}_{Z,r}[f_{w_2}(g_{\theta_2}(\mathbf{Z}) + g_{\theta_1}(\mathbf{r}))] \quad (4)$$

$$\mathcal{L}_{\text{cyc}}(\theta_2, \theta_3) \triangleq \mathbb{E}_Z[\|\mathbf{Z} - g_{\theta_3}(g_{\theta_2}(\mathbf{Z}))\|_1]. \quad (5)$$

The loss (3) is for training the first generator-critic pair,  $(g_{\theta_1}, f_{w_1})$ , of which  $g_{\theta_1}$  learns to generate the independent realization of the noise mimicking the patches in  $\mathcal{N} = \{\mathbf{n}^{(j)}\}_{j=1}^N$ , taking the random vector  $\mathbf{r} \sim p(\mathbf{r})$  as input. The second loss (4) links the two generators,  $g_{\theta_1}$  and  $g_{\theta_2}$ , with the second critic,  $f_{w_2}$ . The second generator  $g_{\theta_2}$  is intended to generate the underlying (unobserved) “clean” image for the input noisy image  $\mathbf{Z}$ , and the critic  $f_{w_2}$  determines how close the distribution of the generated noisy images,  $g_{\theta_2}(\mathbf{Z}) + g_{\theta_1}(\mathbf{r})$ , is to the distribution of the input noisy images. Note by adding the “estimated” clean image with the generated noise from the first generator, we aim to simulate the noisy images that have the independent noise realization of the noise in the original noisy image  $\mathbf{Z}$ . The given noisy images in  $\mathcal{D} = \{\mathbf{Z}^{(i)}\}_{i=1}^n$  are used as input to  $g_{\theta_2}$  as well as to  $f_{w_2}$  in this loss term. The third loss (5) is similar to the so-called cycle loss proposed in CycleGAN, and it works as a “regularizer” for the estimated clean image,  $g_{\theta_2}(\mathbf{Z})$ . In CycleGAN, such loss was devised to impose the cycle consistency between the images such that only the intended characteristic of the input is changed while the basic structure is preserved. We apply this loss to change the noise realization, the “intended characteristic”, while preserving the underlying clean image, the “basic structure”. We show in our experiment that using this third loss plays a critical role in maintaining the quality of the estimated clean image  $g_{\theta_2}(\mathbf{Z})$ .

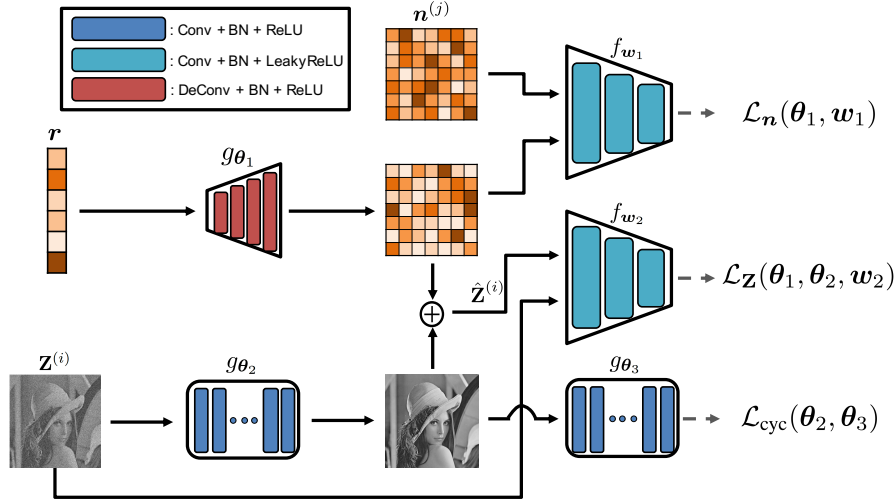


Figure 1: W-GAN based generative model for simulating noisy images

Once the loss functions are defined, training the generators and critics are done in an alternative manner, as in the standard training of W-GAN [1], to approximately solve

$$\min_{\theta_1, \theta_2, \theta_3} \max_{w_1, w_2} \left[ \alpha \mathcal{L}_n(\theta_1, w_1) + \beta \mathcal{L}_Z(\theta_1, \theta_2, w_2) + \gamma \mathcal{L}_{\text{cyc}}(\theta_2, \theta_3) \right], \quad (6)$$

in which  $(\alpha, \beta, \gamma)$  are hyperparameters to control the trade-offs between the loss functions. There are a few important subtle points for training with the overall objective (6). Firstly, while we use

$(\alpha, \beta, \gamma) = (1, 1, 0)$  for the inner maximization for critics, we use  $(\alpha, \beta, \gamma) = (5, 1, 10)$  for the outer minimization for generators. The main intuition for using different  $(\alpha, \beta, \gamma)$  for training the generators is due to different levels of confidence in the generator loss terms. Namely, we assign the largest weight to (5) since it is a deterministic loss and its value has a clear meaning. The generator loss (3), which is in the form of standard W-GAN loss, gets the medium level weight since the meaning of its value is less certain than (5). In contrast, the generator loss in (4), which consists of two generators, can become somewhat unstable during training, hence, it gets the least weight. Secondly, the output layer of  $g_{\theta_2}$  must have the sigmoid activation function. Note  $g_{\theta_2}$  itself can be thought of another denoiser, but since we are not training it with any target, we need to ensure the outputs of  $g_{\theta_2}$  have values between  $[0, 1]$  to prevent from obvious errors of generating negative or too large pixel values. Without the sigmoid activation, it turned out all the generators cannot be trained properly at all. Finally, using the right architectures for the generators and critics, *e.g.*, number of layers and filters, was critical since the training procedure got very sensitive to the architectural variations. The complete details of model architectures and hyperparameter settings is in the Supplementary Material.

### 3.2.3 Iterative GAN2GAN training of a denoiser

Once the training of our W-GAN is done, for each given  $\mathbf{Z}^{(i)}$  in  $\mathcal{D}$ , we can generate the pairs

$$(\hat{\mathbf{Z}}_1^{(i)}, \hat{\mathbf{Z}}_2^{(i)}) = (g_{\theta_2}(\mathbf{Z}^{(i)}) + g_{\theta_1}(\mathbf{r}_1), g_{\theta_2}(\mathbf{Z}^{(i)}) + g_{\theta_1}(\mathbf{r}_2)), \quad (7)$$

in which  $\mathbf{r}_1, \mathbf{r}_2 \in \mathbb{R}^{128}$  are two independent random vectors sampled from  $\mathcal{N}(\mathbf{0}, I)$ . We denote the set of such *generated* noisy image pairs as  $\hat{\mathcal{D}} = \{(\hat{\mathbf{Z}}_1^{(i)}, \hat{\mathbf{Z}}_2^{(i)})\}_{i=1}^n$ . Then, using  $\hat{\mathcal{D}}$ , we can train a CNN-based denoiser  $\hat{X}_{\theta}(\mathbf{Z})$  by employing the usual N2N training that minimizes the following loss,

$$\mathcal{L}_{\text{N2N}}(\theta, \hat{\mathcal{D}}) \triangleq \frac{1}{n} \sum_{i=1}^n \left( \hat{\mathbf{Z}}_1^{(i)} - \hat{X}_{\theta}(\hat{\mathbf{Z}}_2^{(i)}) \right)^2. \quad (8)$$

Note in (8), we only use the generated noisy images and do *not* use the actual observed  $\mathbf{Z}^{(i)}$  in  $\mathcal{D}$ , justifying the name GAN2GAN. While we show in our experimental results that the denoiser obtained by minimizing (8), denoted as  $\hat{X}_{\theta}(\mathbf{Z})$ , is already a decent denoiser, we can in fact devise an iterative GAN2GAN training to further upgrade the obtained  $\hat{X}_{\theta}(\mathbf{Z})$ . Namely, by observing that our second generator in Section 3.2.2,  $g_{\theta_2}$ , is designed to be a denoiser itself, we can replace it with a better quality denoiser,  $\hat{X}_{\hat{\theta}}(\mathbf{Z})$ . Then, for each  $\mathbf{Z}^{(i)}$  in  $\mathcal{D}$ , we can again generate

$$(\tilde{\mathbf{Z}}_1^{(i)}, \tilde{\mathbf{Z}}_2^{(i)}) = (\hat{X}_{\hat{\theta}}(\mathbf{Z}^{(i)}) + g_{\theta_1}(\mathbf{r}_1), \hat{X}_{\hat{\theta}}(\mathbf{Z}^{(i)}) + g_{\theta_1}(\mathbf{r}_2)), \quad (9)$$

to obtain a new set of generated image pairs  $\tilde{\mathcal{D}} = \{(\tilde{\mathbf{Z}}_1^{(i)}, \tilde{\mathbf{Z}}_2^{(i)})\}_{i=1}^n$ . We expect (9) would be closer to the true independently realized noisy image pairs in distribution compared to (7) since a better generator is used. With  $\tilde{\mathcal{D}}$ , the GAN2GAN training, warm starting from  $\hat{X}_{\theta}(\mathbf{Z})$ , can be done again to further fine-tune the model. We show this iterative GAN2GAN training, typically with just one iteration, becomes extremely effective and gives a significant boost in the denoising performance.

## 4 Experimental results

### 4.1 Data and experimental settings

**Data** We used BSD400 [18], a commonly used database, as a source of obtaining the noisy training images. Moreover, to evaluate the effect of the increased data size, we additionally used 1000 noisy images from LabelME [19], particularly for the smooth noisy patch extraction and the W-GAN training. (For the iterative GAN2GAN training, we always used noisy images only from BSD400.) For evaluating the denoising performance, we used the standard benchmark BSD68, which is not included in BSD400.

**Training details** For the smooth noisy patch extraction in Section 3.2.1, we used the patch size of  $96 \times 96$  and generated the noisy image and noise patches,  $\mathcal{D}$  and  $\mathcal{N}$ , respectively. The number of patches in each set was  $n = N = 100,000$  when using LabelME and  $n = N = 20,000$  when only using BSD400. Different  $\lambda$ 's were used for different noise types. For the W-GAN training, we randomly cropped the generated patches to the size of  $64 \times 64$ , and the data augmentation was

done by flipping the patches horizontally and vertically. For the iterative GAN2GAN training, noisy images only from BSD400 are used and the patch size was  $120 \times 120$ ,  $n = 20, 500$ . The same data augmentation as in W-GAN training was done. Moreover, for every minibatch in the GAN2GAN training, we generated new synthetic noisy image pairs using our W-GAN as was done in the noise augmentation of [23]. The architectural details of the generators,  $g_{\theta_1}, g_{\theta_2}, g_{\theta_3}$ , the critics,  $f_{w_1}, f_{w_2}$ , and the final GAN2GAN denoiser,  $\hat{X}_{\theta}(\mathbf{Z})$ , as well as all hyperparameters are given in the Supplementary Material. Of note is that we set the architecture of  $\hat{X}_{\theta}(\mathbf{Z})$  identical to that of DnCNN in [23] to make a fair comparison.

**Comparing methods** The baselines we used are BM3D [6], DnCNN-S/B [25], Noise2Noise (N2N) [14] and Noise2Void (N2V) [12]. We reproduced and trained DnCNN-S/B, N2N and N2V using the publicly available source codes on the *exactly* same training data: BSD400 with the same patch size and number of patches as our GAN2GAN trained  $\hat{X}_{\theta}$ . For *blindly* training DnCNN-B and N2N, we used 20-layers DnCNN model with composite additive white Gaussian noise with  $\sigma \in [0, 55]$ . DnCNN-S/B require the clean target images for training, while N2N requires two independent noisy image pairs. BM3D does not require any additional training, but requires to know  $\sigma$ . N2V deals with the same setting as our GAN2GAN, and has the U-net architecture as given in [12].

## 4.2 Denoising results

**White Gaussian noise** Table 1 shows the PSNR/SSIM results on BSD68 corrupted by white Gaussian noise with different  $\sigma$  values. We report four variations of our GAN2GAN method (denoted as G2G from now on for brevity). G2G(BSD) corresponds to the denoiser that only uses BSD400 for all three steps and no iterative training in Section 3.2.3 is done, and G2G<sub>I</sub>(BSD) stands for the same scheme but with one additional iteration. Moreover, G2G(LM,BSD) stands for the denoiser that uses LabelME extracted patches for training W-GAN and uses BSD400 for the GAN2GAN training without any iteration, and G2G<sub>I</sub>(LM,BSD) is the same scheme as G2G (LM,BSD) with one iteration.

Table 1: Results on *BSD68/Gaussian*. Boldface denotes the best among the GAN2GAN variations.

| PSNR /SSIM  | BM3D             | DnCNN-S          | DnCNN-B          | N2N              | N2V              | G2G (BSD)        | G2G <sub>I</sub> (BSD)         | G2G (LM,BSD)     | G2G <sub>I</sub> (LM,BSD)      |
|-------------|------------------|------------------|------------------|------------------|------------------|------------------|--------------------------------|------------------|--------------------------------|
| $\sigma=15$ | 31.07<br>/0.8717 | 31.54<br>/0.8848 | 31.14<br>/0.8689 | 31.22<br>/0.8793 | 28.32<br>/0.7883 | 30.98<br>/0.8552 | <b>31.51</b><br><b>/0.8827</b> | 31.27<br>/0.8700 | <b>31.55</b><br><b>/0.8826</b> |
| $\sigma=25$ | 28.56<br>/0.8013 | 29.03<br>/0.8167 | 28.84<br>/0.8132 | 28.82<br>/0.8132 | 26.69<br>/0.7093 | 28.23<br>/0.7669 | 28.82<br>0.8056                | 28.65<br>/0.7901 | <b>28.93</b><br><b>0.8079</b>  |
| $\sigma=30$ | 27.74<br>/0.7727 | 28.13<br>/0.7860 | 27.99<br>/0.7857 | 27.95<br>/0.7824 | 26.31<br>/0.6901 | 27.58<br>/0.7413 | <b>27.99</b><br><b>/0.7783</b> | 27.80<br>/0.7591 | 27.96<br>/0.7724               |
| $\sigma=50$ | 25.60<br>/0.6866 | 26.04<br>/0.6967 | 25.15<br>/0.6330 | 24.49<br>/0.5890 | 24.58<br>/0.5944 | 25.08<br>/0.6215 | 25.55<br>/0.6639               | 25.47<br>/0.6542 | <b>25.73</b><br><b>/0.6790</b> |

From the table, we can make following observations. Firstly, we see our G2G (BSD) already significantly outperforms N2V, which is trained on the exact same dataset. Moreover, we observe that when the training data size for W-GAN training increases, the performance improves as in G2G (LM,BSD). Secondly, the iterative G2G training certainly helps to boost the PSNR performance for about 0.3 ~ 0.5dB by comparing G2G<sub>I</sub> schemes with their counterparts. It turns out to be more helpful when the training data size for W-GAN is smaller (i.e., for BSD400 only case), and the performance gap between the no iteration schemes due to the training data size can be mostly closed via the iterative training. More analyses on the data size and iterative training is given in the ablation study. Thirdly, the denoising performance of G2G<sub>I</sub> (BSD) becomes *very* strong that it even outperforms the blindly trained DnCNN-B and N2N, which have access to either clean target images or the two independently realized noisy pairs. This result may seem somewhat counterintuitive since our G2G has significantly less information. We believe the main reason for such result is due to the accurate noise estimation and generation capability of our W-GAN; that is, while DnCNN-B and N2N are trained with the composite noise levels, our G2G can accurately estimate the right noise level and train for the particular noise level. We verify this point in our ablation study section. Finally, when  $\sigma$  is small, G2G<sub>I</sub> (LM,BSD) can even outperform DnCNN-S, which knows the correct noise  $\sigma$  and has access to the clean target images. This somewhat surprising result may be due to the increased training dataset using LabelME and the capability of our W-GAN effectively learning the information about underlying clean images.

**Mixture and correlated noise** Table 2 shows the results for the noise beyond the white Gaussian noise. Note our G2G does not assume any distributional or correlation structure of the noise, hence it can still run as before for the noise different from Gaussian or the noise with non-diagonal covariance matrix. In Table 2, the G2G results are for using (LM,BSD) as specified above. Moreover, DnCNN-B and N2N are still the ones blindly trained with the white Gaussian noise.

For mixture noise, we tested with two cases. Case A corresponds to the same setting as given in [5], i.e., 70% Gaussian  $N(0, 0.01)$ , 20% Gaussian  $N(0, 1)$ , and 10% Uniform  $[-s, s]$  with  $s = 15, 25$ . For case B, we tested with larger noise variances, i.e., 70% Gaussian  $N(0, 15)$ , 20% Gaussian  $N(0, 25)$ , and 10% Uniform  $[-s, s]$  with  $s = 30, 50$ . From the table, we first note that DnCNN-B and N2N, which are only trained with white Gaussians, suffer from performance degradation due to the 10% mixture of uniform noise. The the conventional BM3D outperforms them in this case. However, our G2G<sub>I</sub> can still denoise very well by accurately learning and generating the actual noise in the data and outperforms all the baselines. Note N2V suffers very much, and the results are not comparable to ours. Note also that GCBD [5] trains with the clean target images with similar noise generative model using the rule (1), but G2G outperforms it with only using noisy images. This result confirms the effectiveness of the learning and training of our G2G framework.

Table 2: Results on *BSD68/Mixture and Correlated noise*. Boldface denotes the best among all.

|                  |                     | PSNR<br>/SSIM | BM3D             | DnCNN-B          | N2N              | N2V              | GCBD        | G2G              | G2G <sub>I</sub>               |
|------------------|---------------------|---------------|------------------|------------------|------------------|------------------|-------------|------------------|--------------------------------|
| Mixture<br>Noise | Case A              | s=15          | 41.44<br>/0.9822 | 38.95<br>/0.9687 | 39.81<br>/0.9737 | 31.90<br>/0.9087 | 42.00<br>/- | 42.55<br>/0.9881 | <b>42.90</b><br><b>/0.9900</b> |
|                  |                     | s=25          | 37.97<br>/0.9647 | 36.97<br>/0.9555 | 37.12<br>/0.9589 | 31.05<br>/0.8909 | 39.87<br>/- | 39.99<br>/0.9827 | <b>40.30</b><br><b>/0.9845</b> |
|                  | Case B              | s=30          | 30.12<br>/0.8496 | 30.39<br>/0.8549 | 30.38<br>/0.8607 | 27.85<br>/0.7679 | -           | 30.37<br>/0.8456 | <b>30.66</b><br><b>/0.8606</b> |
|                  |                     | s=50          | 29.27<br>/0.8190 | 30.05<br>/0.8474 | 30.03<br>/0.8507 | 23.48<br>/0.5157 | -           | 29.93<br>/0.8330 | <b>30.16</b><br><b>/0.8491</b> |
|                  | Correlated<br>Noise | σ=15          | 29.84<br>/0.8504 | 30.71<br>/0.8916 | 30.66<br>/0.8950 | 27.98<br>/0.8046 | -           | 30.88<br>/0.8879 | <b>31.41</b><br><b>/0.8890</b> |
|                  |                     | σ=25          | 26.69<br>/0.7544 | 27.36<br>/0.8225 | 27.31<br>/0.8234 | 25.76<br>/0.7237 | -           | 27.38<br>/0.8007 | <b>27.85</b><br><b>/0.9017</b> |

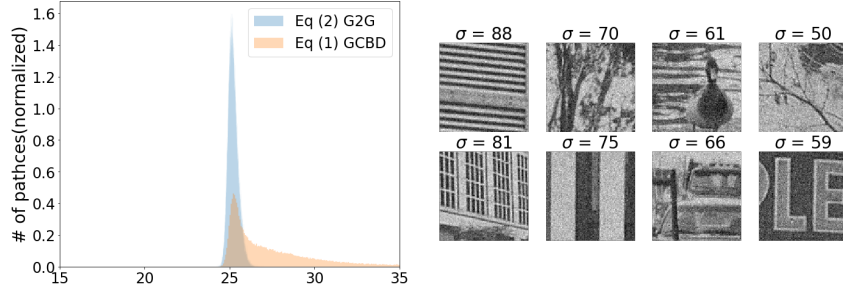
For correlated noise, we generated the following noise for each  $\ell$ -th pixel

$$N_\ell = \eta M_\ell + (1 - \eta) \left( \frac{1}{\sqrt{|\mathcal{NB}_\ell|}} \sum_{m \in \mathcal{NB}_\ell} M_m \right), \quad \ell = 1, 2, \dots \quad (10)$$

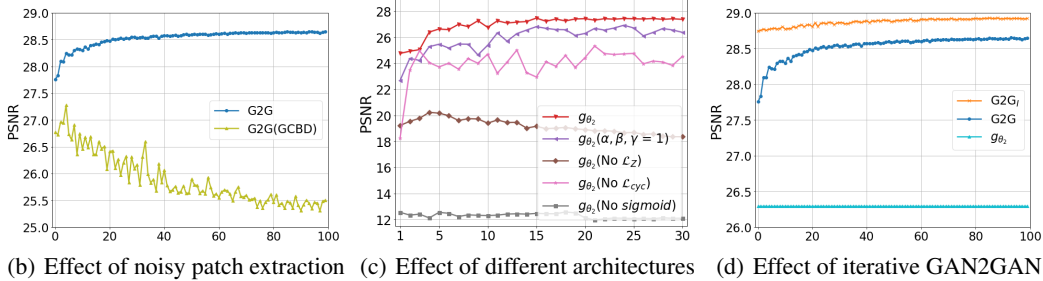
in which  $\{M_\ell\}$  are white Gaussian  $\mathcal{N}(0, \sigma^2)$ ,  $\mathcal{NB}_\ell$  are the  $k \times k$  neighborhood patch except for the pixel  $\ell$ , and  $\eta$  is a mixture parameter. We set  $\eta = 1/\sqrt{2}$  such that the marginal distribution of  $N_\ell$  is also  $\mathcal{N}(0, \sigma^2)$  and set  $k = 16$ . Note in this case,  $N_\ell$  has a spatial correlation structure. We tested with  $\sigma = 15, 25$ . From Table 2, we first see that the PSNRs of DnCNN-B and N2N again significantly drop compared to those for the same  $\sigma$ 's in Table 1 due to the noise distribution mismatch. In contrast, G2G already outperform them solely learning from the single noisy images, and the iterative version, G2G<sub>I</sub>, achieves 0.5~0.7dB gains over them. Again, the results of N2V are not comparable to ours.

### 4.3 Ablation Study

**Smooth noisy patch extraction** Figure 2(a) compares the result of the smooth noisy patch extraction using (1) of GCBD [5] and our (2), on the LabelME images corrupted by white Gaussian noise with  $\sigma = 25$ . The histogram shows the distributions of the empirical  $\sigma$ 's computed from the patches extracted by the two rules, respectively. We clearly see while our method extracts patches with empirical  $\sigma$  highly concentrated on the true one, the rule (1) generates patches with much larger variations. Moreover, the visualization on the right shows some extreme patches extracted by the rule (1), which clearly are far from being smooth. Figure 2(b) further shows the effect of smooth noisy patch extraction on the final G2G training by plotting the PSNR curve on BSD68 as the training using (8) continues. We clearly see that the PSNR of G2G training using the synthetic noisy image pairs, which are generated from the W-GAN trained with the patches extracted by the rule (2), converges nicely as the G2G iteration increases. However, for G2G (GCBD), which stands for training the W-GAN with noisy patches extracted by the GCBD rule (1), the PSNR keeps decreasing showing the denoiser training is not happening properly.



(a) Comparison of the smooth noisy patch extraction rule for Gaussian noise with  $\sigma = 25$ .



(b) Effect of noisy patch extraction (c) Effect of different architectures (d) Effect of iterative GAN2GAN

Figure 2: Ablation study results. (b),(c), and (d) show PSNR on BSD68/Gaussian noise ( $\sigma = 25$ ).

**Architectural variations for W-GAN** Figure 2(c) shows the PSNRs of the second generator,  $g_{\theta_2}$ , on BSD68 trained with different W-GAN architectures. The horizontal axis stands for the W-GAN training epochs. Recall  $g_{\theta_2}$  is also designed to be a denoiser. We tested with four variations; “ $(\alpha, \beta, \gamma=1)$ ” stands for the different hyperparameter setting when training the generators using (6), “No  $\mathcal{L}_Z$ ” stands for the case with no second critic  $f_{w_2}$ , “No  $\mathcal{L}_{cyc}$ ” stands for the case with no cyclic loss (5), and “No sigmoid” stands for not using the sigmoid activation at the output layer of  $g_{\theta_2}$ . We first confirm that our proposed architecture achieves the highest PSNR for  $g_{\theta_2}$ . We also confirm that the sigmoid activation and the second critic (which appears in the  $\mathcal{L}_Z$  loss 4) are essential, as the PSNR of  $g_{\theta_2}$  significantly drops without them. The cyclic loss (5) as well as the right setting of  $(\alpha, \beta, \gamma)$  are also very important. Achieving a decent PSNR for  $g_{\theta_2}$  is critical, as it affects the quality of the simulated noisy images used for the G2G training.

**Iterative GAN2GAN training** Figure 2(d) clearly shows the PSNR gain of the iterative G2G training. As observed in Table 1, the additional 0.3~0.4dB PSNR boost that  $G2G_I$  brings was essential in even outperforming DnCNN-B or N2N. In Table 3, we also show the effect of training data size for W-GAN, in which 100% stands for the full data setting we used with LabelME data. From the table, we observe that the 1dB PSNR gap of  $g_{\theta_2}$ ’s for 25% and 100% training data close down to 0.1dB for  $G2G_I$ . This shows the data efficient nature of our  $G2G_I$ , which could become very useful in practical applications with small amount of data.

Table 3: PSNR(dB) on *BSD68/Gaussian* ( $\sigma = 25$ ) with varying data size for training our W-GAN.

| Data size | $g_{\theta_2}$ | G2G   | G2G <sub>I</sub> |
|-----------|----------------|-------|------------------|
| 25%       | 25.36          | 28.48 | <b>28.83</b>     |
| 50%       | 26.12          | 28.55 | <b>28.79</b>     |
| 75%       | 26.21          | 28.65 | <b>28.87</b>     |
| 100%      | 26.30          | 28.65 | <b>28.93</b>     |

## 5 Conclusion

We proposed a novel GAN2GAN method, which can tackle the challenging blind image denoising problem solely with single noisy images. Our method showed impressive denoising performance that even sometimes outperformed the methods that have more information, such as clean target images. Our future work includes applying GAN2GAN to the real-world blind denoising and extend our method to source dependent noise distributions.



## References

- [1] Martin Arjovsky, Soumith Chintala, and Léon Bottou. Wasserstein generative adversarial networks. In *International Conference on Machine Learning*, pages 214–223, 2017.
- [2] Joshua Batson and Loic Royer. Noise2self: Blind denoising by self-supervision. *arXiv preprint arXiv:1901.11365*, 2019.
- [3] A. Buades, B. Coll, and J. M. Morel. A review of image denoising algorithms, with a new one. *SIAM Journal on Multiscale Modeling and Simulation: A SIAM Interdisciplinary Journal*, 2005.
- [4] Sungmin Cha and Taesup Moon. Fully convolutional pixel adaptive image denoiser. *arXiv preprint arXiv:1807.07569*, 2018.
- [5] Jingwen Chen, Jiawei Chen, Hongyang Chao, and Ming Yang. Image blind denoising with generative adversarial network based noise modeling. In *Proceedings of the IEEE Conference on Computer Vision and Pattern Recognition*, pages 3155–3164, 2018.
- [6] K. Dabov, A. Foi, V. Katkovnik, and K. Egiazarian. Image denoising by sparse 3-d transform-domain collaborative filtering. *IEEE Trans. Image Processing*, 16(8):2080–2095, 2007.
- [7] D. Donoho and I. Johnstone. Adapting to unknown smoothness via wavelet shrinkage. *Journal of American Statistical Association*, 90(432):1200–1224, 1995.
- [8] M. Elad and M. Aharon. Image denoising via sparse and redundant representations over learned dictionaries. *IEEE Trans. Image Processing*, 54(12):3736–3745, 2006.
- [9] Ian Goodfellow, Jean Pouget-Abadie, Mehdi Mirza, Bing Xu, David Warde-Farley, Sherjil Ozair, Aaron Courville, and Yoshua Bengio. Generative adversarial nets. In *Advances in neural information processing systems*, pages 2672–2680, 2014.
- [10] S. Gu, L. Zhang, W. Zuo, and X. Feng. Weighted nuclear norm minimization with applications to image denoising. In *Computer Vision and Pattern Recognition (CVPR)*, 2014.
- [11] V. Jain and H.S. Seung. Natural image denoising with convolutional networks. In *NIPS*, 2008.
- [12] Alexander Krull, Tim-Oliver Buchholz, and Florian Jug. Noise2void-learning denoising from single noisy images. *arXiv preprint arXiv:1811.10980*, 2018.
- [13] Jaakko Lehtinen, Jacob Munkberg, Jon Hasselgren, Samuli Laine, Tero Karras, Miika Aittala, and Timo Aila. Noise2Noise: Learning image restoration without clean data. In *ICML*, 2018.
- [14] Jaakko Lehtinen, Jacob Munkberg, Jon Hasselgren, Samuli Laine, Tero Karras, Miika Aittala, and Timo Aila. Noise2noise: Learning image restoration without clean data. In *International Conference on Machine Learning*, pages 2971–2980, 2018.
- [15] Ding Liu, Bihan Wen, Yuchen Fan, Chen C. Loy, and Thomas S. Huang. Non-local recurrent network for image restoration. In *NIPS*, 2018.
- [16] S. Lunz, O. Öktem, and C.-B. Schönlieb. Adversarial regularizers in inverse problems. In *NIPS*, 2018.
- [17] J. Mairal, F. Bach, J. Ponce, G. Sapiro, and A. Zisserman. Non-local sparse models for image restoration. In *International Conference on Computer Vision (ICCV)*, 2009.
- [18] D. Martin, C. Fowlkes, D. Tal, and J. Malik. A database of human segmented natural images and its application to evaluating segmentation algorithms and measuring ecological statistics. In *Proc. 8th Int’l Conf. Computer Vision*, volume 2, pages 416–423, July 2001.
- [19] Bryan C Russell, Antonio Torralba, Kevin P Murphy, and William T Freeman. Labelme: a database and web-based tool for image annotation. *International journal of computer vision*, 77(1-3):157–173, 2008.
- [20] Ying Tai, Jian Yang, Xiaoming Liu, and Chunyan Xu. Memnet: A persistent memory network for image restoration. In *ICCV*, 2017.
- [21] Dmitry Ulyanov, Andrea Vedaldi, and Victor Lempitsky. Deep image prior. In *CVPR*, 2018.
- [22] R.A. Yeh, T. Y. Lim, C. Chen, A. G. Schwing, M. Hasegawa-Johnson, and M. N. Do. Image restoration with deep generative models. In *ICASSP*, 2018.
- [23] K. Zhang, W. Zuo, Y. Chen, D. Meng, and L. Zhang. Beyond a gaussian denoiser: Residual learning of deep cnn for image denoising. *IEEE Trans. Image Processing*, 26(7):3142 – 3155, 2017.

- [24] Xiaoshuai Zhang, Yiping Lu, Jiaying Liu, and Bin Dong. Dynamically unfolding recurrent restorer: A moving endpoint control method for image restoration. *arXiv preprint arXiv:1805.07709*, 2018.
- [25] Yulun Zhang, Yapeng Tian, Yu Kong, Bineng Zhong, and Yun Fu. Residual dense network for image restoration. *arXiv preprint arXiv:1812.10477*, 2018.
- [26] Jun-Yan Zhu, Taesung Park, Phillip Isola, and Alexei A Efros. Unpaired image-to-image translation using cycle-consistent adversarial networks. In *Proceedings of the IEEE international conference on computer vision*, pages 2223–2232, 2017.
- [27] D. Zoran and Y. Weiss. From learning models of natural image patches to whole image restoration. *International Conference on Computer Vision (ICCV)*, 2011.

---

# Supplementary Materials for GAN2GAN: Generative Noise Learning for Blind Image Denoising with Single Noisy Image

---

## 1 Details on experiments

### 1.1 Details on a noise extraction

Table 1:  $\lambda$  for the noise extraction

|           | Gaussian noise | Mixture noise | Correlated noise |
|-----------|----------------|---------------|------------------|
| $\lambda$ | 0.03           | 0.1           | 0.15             |

To extract noise patches using our noise patch extraction algorithm, we used a different  $\lambda$  depending on the type of noise. Figure 1 shows  $\lambda$  we are used.

### 1.2 Details on training W-GAN

Table 2: Details on Generator ( $g_{\theta_1}$ )

| Input shape : ( $r$ ,)                     |                           | Details of DeConv layer |                |             |        |         |
|--|---------------------------|-------------------------|----------------|-------------|--------|---------|
| Layer Num                                  | Layer composition         | Input channel           | Output channel | Kernel size | Stride | Padding |
| 1  | DeConv + BatchNorm + ReLU | $r$                     | 64             | 4           | 1      | 0       |
| 2  | DeConv + BatchNorm + ReLU | 64                      | 32             | 4           | 2      | 1       |
| 3  | DeConv + BatchNorm + ReLU | 32                      | 16             | 4           | 2      | 1       |
| 4  | DeConv + BatchNorm + ReLU | 16                      | 8              | 4           | 1      | 1       |
| 5  | Conv + Tanh               | 8                       | $C$            | 4           | 2      | 1       |
| Output shape : ( $64 \times 64 \times C$ ) |                           | -                       |                |             |        |         |

Tables 2 show the details on Generator we used for generating a noise.  $r$  is a random vector to generate a noise patch from  $g_{\theta_1}$  and  $C$  is the channel of image.  $g_{\theta_2}$  and  $g_{\theta_3}$  in our W-GAN are equal to DnCNN model, however,  $g_{\theta_3}$  has 15 layers and sigmoid activation in output layer. We also used Critic in Figure 3 for training W-GAN. In the process of training W-GAN, we used Adam optimizer for the generators and RMSProp optimizer for the discriminators. The initial learning rate for Adam is 0.0004 and for RMSProp is 0.00005. Also, learning rate decay, which drop the learning rate linearly starting from 10 epochs, is applied to Adam optimizer. the clipping value for the discriminator is set to 0.02 and critic iteration is 5. We trained W-GAN model for 30 epochs with mini-batch size 64.

### 1.3 Details on training GAN2GAN

We trained DnCNN with 17-layers using GAN2GAN and Adam optimizer with initial learning of 0.001. Learning rate schedule, which is lower the learning rate by half every 20epochs, is applied to Adam optimizer. The training epochs of GAN2GAN is 100 and mini-batch size is 4.

Table 3: Details on Critic ( $f_{w_1}, f_{w_2}$ )

| Input shape : (64x64xC)  |                              | Details of Conv layer |                |             |        |         | Details of LeakyReLU |
|--------------------------|------------------------------|-----------------------|----------------|-------------|--------|---------|----------------------|
| Layer Num                | Layer composition            | Input channel         | Output channel | Kernel size | Stride | Padding | Alpha                |
| 1                        | Conv + BatchNorm + LeakyReLU | C                     | 128            | 4           | 2      | 1       | 0.2                  |
| 2                        | Conv + BatchNorm + LeakyReLU | 128                   | 256            | 4           | 2      | 1       |                      |
| 3                        | Conv + BatchNorm + LeakyReLU | 256                   | 512            | 4           | 2      | 1       |                      |
| 4                        | Conv                         | 512                   | 1              | 4           | 1      | 0       | -                    |
| Output shape : (64x64x1) |                              | -                     |                |             |        |         | -                    |

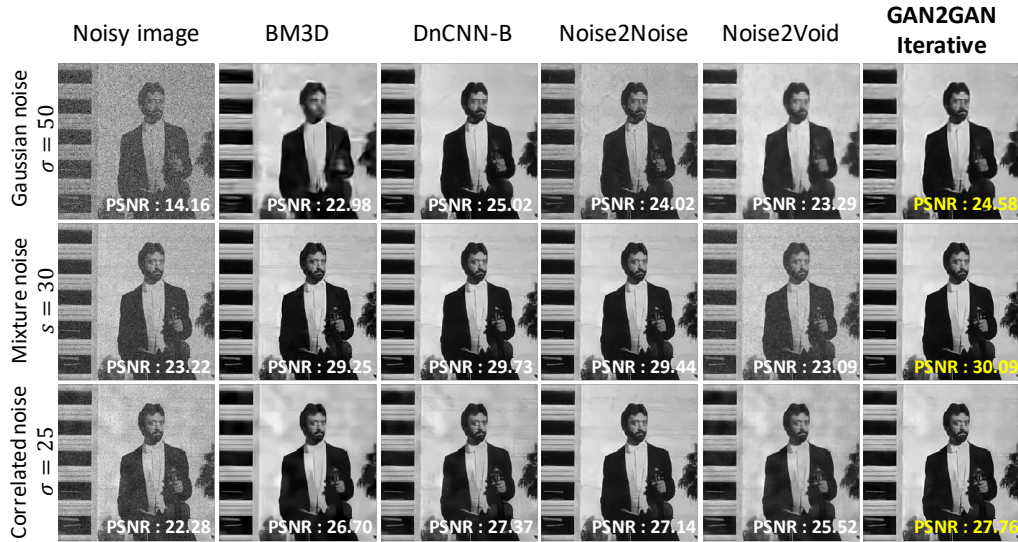


Figure 1: Visualizations

## 2 Visualizations

We visualize denoised images of different type of noise in Figure 1. We cropped an equal location of the denoised images from baselines and experiments. From noisy images, we can see that the pattern of three type of noise is different. Overall, the visualization of GAN2GAN Iterative looks the best compared to other baselines. Note that we only used noisy images as a training data and only Noise2Void assumed the same situation.